International Journal of Innovative Technology and Exploring Engineering (IJITEE)
ISSN: 2278-3075 (Online), Volume-14 Issue-10, September 2025

Kalman Filter for an Industrial Tower Crane Controlled in Closed-Loop with Anti-Sway Profile

Roberto P. L. Caporali

Abstract: ***This paper presents a method for generating a velocity profile for an industrial tower crane controlled in a closed-loop anti-sway system. We obtain, as a final result of the theory developed here, the Kalman Observer for the Tower Crane System considered. In this paper, we introduce an iterative procedure for the Kalman-Bucy observer, creating a new method for controlling a Tower Crane in a closed-loop system. We introduce the use of a Kalman filter to reduce the errors introduced by both the model approximation for Anti-Sway control and, on the other hand, measurement errors due to the sensors used in the closed-loop control. Therefore, this application is characterized by the union of two fundamental factors: the control of load swing during jib rotation and the use of the Kalman filter algorithm to correct the errors obtained in closed-loop control. In this work, we describe in detail the Lagrange equations for defining the swaying effect on the jib's rotational motion and thus arrive at the iterative equations for calculating the jib's motion itself. We analyse the characteristics of the Kalman Filter in general, which, as a consequence, leads to defining the Matrix Equation of the Kalman Filter for the Jib Crane. We simulate the time evolution of the motion equations and define the input red from the input sensors randomly. We represent three Velocity Profiles: the theoretical Velocity reference profile of the Slewing, the profile of the Slewing considering both the measurement noise and the noise due to the modelling error of the phenomenon, and, finally, the profile of the Slewing output, obtained by filtering the signals through the Kalman filter. It is observed that, as the variances of the random phenomena considered decrease, an increasingly smooth trend of the profiles themselves is observed.***

Keywords**: *Kalman Filter, Tower Crane, Anti-Sway, Closed-loop Control.***

Abbreviations:
DOF: Degree Of Freedom
FEM: Finite Element Analysis
IMU: Inertial Measurements Unit

I. INTRODUCTION

In this work, we study the controlled movement of a Slewing crane, specifically an Industrial Tower Crane, characterised by being equipped with sensors to measure the position/speed of rotation and the movement of the trolley.

Manuscript received on 22 August 2025 | First Revised Manuscript received on 27 August 2025 | Second Revised Manuscript received on 03 September 2025 | Manuscript Accepted on 15 September 2025 | Manuscript published on 30 September 2025.
*Correspondence Author(s)
Roberto P. L. Caporali*, Department of Mathematics for Applied Physics, Roberto Caporali, Imola, BO, Italy. Email ID: robertopaolo.caporali@gmail.com, ORCID ID: 0000-0001-9492-0315

© The Authors. Published by Blue Eyes Intelligence Engineering and Sciences Publication (BEIESP). This is an open-access article under the CC-BY-NC-ND license http://creativecommons.org/licenses/by-nc-nd/4.0/

This system is characterised as a closed-loop control system. Tower Cranes are used to move construction materials and, typically, are manually controlled by expert operators. However, increasingly, functions are being introduced that allow these types of Cranes to carry out movement operations automatically ([1]). This type of automatic operation on Tower Cranes is, in general, much more complex than those that occur for Industrial Overhead or Gantry Cranes. This is due to both the fact that Tower Cranes operate outdoors and are therefore exposed to variable weather conditions, and the fact that their structure is flexible and thus subject to deformations.

In contrast to the Industrial Overhead cranes, which have a one-degree-of-freedom sway in the solution equations, Slewing cranes, such as Tower cranes or self-erecting cranes, undergo rotation of the Jib. Therefore, the equations of motion must be coupled.

A large number of works have been developed regarding the controlled motion of slewing tower cranes. Among the most recent works, we can mention the study by Alfadhli et al. [2], in which they define a smooth command input to achieve zero payload oscillations with simultaneous radial and slewing motions of the tower crane. In the paper by Montonen et al. [3], a combination of Input Shaping and Sway control was developed, resulting in slewing control for a tower crane. In recent work by Zhang et al. [4], a payload sway reduction method for 4-DOF tower cranes was defined based on an adaptive integral control approach. Furthermore, in the recent work of Li et al. [5], they defined a method for Anti-sway Trajectory control of a Double-pendulum Tower Crane using an Evolutionary Algorithm. The author of this work has also recently developed techniques for the open-loop control of tower cranes. In the paper [6], he described an iterative method for controlling the sway of a payload using a command profile system. Instead, in work [7], the method considered was applied to a harbour crane.

The limitation of the works considered above lies in the fact that they are primarily based on applications of open-loop methods, which, in an open environment and therefore conditioned by wind conditions such as those of tower cranes, is a significant limitation. Furthermore, these works do not consider the vibrations of the elastic structure constituted by the tower crane. Such vibrations are taken into account in some of the most recent works on tower cranes. First, in the paper [8], the authors present dynamic models and simulate them to understand the dynamic characteristics and vibration features of the tower cranes. In work [9], Ghawzani et al. define a method to increase the stiffness using reinforcements in the mast modelled using the modal parameters. In FEM analysis, reinforcements are applied in precise positions

Published By:
Blue Eyes Intelligence Engineering and Sciences Publication (BEIESP)
© Copyright: All rights reserved.

along the vertical axes of the tower crane. Paper [10] presents a modal method for slewing control considering a distributed-mass model. The crane jib is defined as an Euler-Bernoulli beam. The author of this work has also published several papers related to the influence of vibrations on the behaviour of tower cranes. In particular, in the first of three papers [11] published in 2021, the author defined some of the fundamental principles governing the influence of vibrations in the elastic structure of the jib crane on the behaviour during rotation of the jib. In the second paper [12], in 2023, the author developed an innovative calculation for determining the normal vibration modes of a Tower jib crane. He used a finite element system to model the jib crane as an Euler-Bernoulli beam. He made the approximation of dividing the boom into a limited number of elements, based on the weight distribution of the different sectors. This allowed us to obtain an approximate analytical solution to the problem. Finally, in the most recent [13], the author developed a method for controlling a tower crane designed as a non-rigid system. In fact, under external excitations, both wanted and non-wanted, the payload tends to sway around its vertical axis, and this motion is coupled to the dynamic vibration of the crane structure.

All these very recent solutions for controlling the tower crane, which also take into account the vibrations due to its elastic structure, overlook a fundamental point. The fact that, if the system is controlled in a closed loop, i.e., using sensors that provide feedback on the relative position, rotation speed, or sway angle, these sensors are subject to measurement noise. Furthermore, a possible error in the position/velocity target defined by the PLC must also be considered, due to the simplifications in the theory used to describe the tower crane's movements through the software. As a consequence, some recent works have introduced the use of the Kalman filter. The Kalman filter is a recursive filter that estimates the state of a variable based on a series of measurements, taking into account noise. Due to its characteristics, it is an excellent filter for noise and disturbances acting on zero-mean Gaussian systems. Pezhman et al. [14] introduced the use of the Kalman filter for the closed-loop control of an overhead crane. Jaehoon et al. [15] also used the Kalman filter for the same application. Instead, both Zhimei et al. [16] and Thomas et al. [17], who have defined position control methods based on the Dempster-Shafer mathematical theory and a Model-based velocity-positioning control for self-erecting tower cranes, respectively, have addressed their applications to tower slewing cranes using different motion control methods. The author of this paper had also defined an application using the Kalman Filter for Overhead Cranes [18], but this application was mainly aimed at systems with quantum control algorithms.

In this paper, we present a closed-loop anti-sway control application for a tower slewing crane. This application is characterised by the union of two fundamental factors: the control of the load swing during jib rotation and the use of the Kalman filter algorithm to correct errors obtained in the closed-loop control. We get a control system that is both easily applicable and precise in eliminating all mistakes derived from the measurements.

In this work, the equations governing sway control are derived using an iterative calculation method. The method employed in this paper utilises a “command smoothing” technique to mitigate sway, which is achieved by incorporating additional damping to counteract sway. Because this method is iterative, we can obtain the total damping of the sway by repeatedly changing the velocity set during the movement of the Jib, even if the previous damping control of the oscillations is still in progress.

Furthermore, the other factor that characterizes this work on tower cranes, and makes it innovative, consists of using the Kalman filter to reduce the errors introduced, on the one hand, by the approximation of the model used to define the position/velocity target profile, and on the other hand, by measurement errors due to the sensors used. The cable angles are estimated using two inertial sensors. One could be installed at the hook block, and the other could be installed at the tower tip.

We have organised this paper in the following manner. In Section II, the equations of motion of the jib are defined and described. From this, the oscillation patterns in the radial and transverse directions to the direction determined by the jib are derived. Subsequently, in Section III, the fundamental characteristics of the Kalman filter are determined. Then, in Section IV, the equations derived from the Kalman filter theory, specifically relating to our case of tower jib crane control, are described. In Section V, an implementation of the method and the most relevant results of the model simulation are presented. At the end, in Section VI, concluding remarks are defined, highlighting possible developments of the work in question.



[Fig.1: Example of a Tower Jib Crane] [18]

II. DYNAMIC MODEL OF THE TOWER CRANE SYSTEM

We can consider the Tower crane as the set of:

1. A vertical flexible column, the Tower.
2. A flexible Jib.
3. A trolley system, a hoisting line, and a payload.
4. φ and l Represent the slew angle and the length of the hoisting line, respectively.
5. The slew angle is the rotating horizontal angle of the crane Jib while the commanded movement is started.

Sway angles are obtained as the crane runs, namely, they are the tangential sway φ_t ,

Published By:
Blue Eyes Intelligence Engineering
and Sciences Publication (BEIESP)
© Copyright: All rights reserved.

and the radial sway φ_r. In this work, we consider the payload as a point mass and assume that it exhibits the behaviour of a pendulum. A geometric description of the Tower Crane system is shown in Fig. 2.

We will refer to the paper by the author of this work [13], where the Dynamic model of the Tower crane is described in detail, without considering the flexibility of the structure.

Referring to work [13] According to the author, the slewing crane can be defined by:

1. A rotating Jib.
2. A translating trolley on the jib.
3. A load cable having a length L.
4. A payload of mass m_L is connected to the trolley with mass $m_{Tr.}$

Besides, we consider the mass of the rope to be small compared to the payload, and therefore, it is neglected.

A. Lagrange Equations for the Swaying Movements

We represent the dynamics of the Tower crane by a mathematical system with five independent degrees of freedom, described by five Lagrangian coordinates q_i :

$q_1 = r$: the radial position of the mass centre of the trolley on the x-axis.

$q_2 = \varphi$: Slewing angle (rotation around the z-axis).

$q_3 = l$: hoisting position of the crane (along the z-axis).

$q_4 = \varphi_x$: sway angle tangential to the radial direction.

$q_5 = \varphi_y$: sway angle normal to the radial direction.

We consider the Lagrange function:

$$L = T - U \quad \dots \quad (1)$$

where T is the Kinetic Energy of the crane system, and U is the Potential Energy. Using the generalized Lagrange equations:

$$\frac{d}{dt}\left(\frac{\partial L}{\partial \dot{q}_i}\right) - \frac{\partial L}{\partial q_i} = Q_i \quad \dots \quad (2)$$

Therefore, we obtain the system of equations in the generalized coordinates q_i.

In the Lagrange equations, the generalised non-conservative Forces Qi are introduced to account for dissipative forces. These forces represent:

1. The components of the wind force and the components of the forces responsible for the rotation movement damping.
2. The components, on the axes x and y, of air resistance forces acting on both the payload and the hoisting system.

Focusing only on the equations relative to $\ddot{\varphi}_x$ and $\ddot{\varphi}_y$ we have:

$$l\ddot{\varphi}_x = \left\{-2\left(\dot{l}\dot{\varphi}_x - l\dot{\varphi}\dot{\varphi}_y\right) - \left(\frac{k_{D,x}}{m_L}\right)\dot{\varphi}_x - k_{E,x}l\varphi_x\right\} + \begin{Bmatrix}\left(l\ddot{\varphi}\varphi_y\right) + l\dot{\varphi}^2\varphi_x - 2\dot{l}\dot{\varphi}\varphi_y \\ -g\varphi_x + \left(\frac{\dot{l}^2}{l}\right)\varphi_x\end{Bmatrix} + \{r\dot{\varphi}^2 - \ddot{r}\} \quad \dots \quad (3)$$

$$l\ddot{\varphi}_y = \left\{-2\left(\dot{l}\dot{\varphi}_y - l\dot{\varphi}\dot{\varphi}_x\right) - \left(\frac{k_{D,y}}{m_L}\right)\dot{\varphi}_y - k_{E,y}l\varphi_y\right\} + \begin{Bmatrix}\left(l\ddot{\varphi}\varphi_x\right) + l\dot{\varphi}^2\varphi_y - 2\dot{l}\dot{\varphi}\varphi_x \\ -g\varphi_y + \left(\frac{\dot{l}^2}{l}\right)\varphi_y\end{Bmatrix} + \{-2\dot{r}\dot{\varphi} - r\ddot{\varphi}\} \quad \dots \quad (4)$$

where $k_{D,x}$ and $k_{D,y}$ are the Damping coefficients in direction x and y, $k_{E,x}$ and $k_{E,y}$ are the Elastic coefficients in direction x and y, m_L is the Load mass, and g is the gravitation acceleration. Considering eq. (3), ϕ_x,

B. Iterative Method for the Solution of Equations

$\dot{\phi}_x$ and $\ddot{\phi}_x$ are calculated with an iterative method that, at any time t, is defined in the following way:

$$\dot{r}_t = (r_t - r_{t-1}) \cdot \Delta t \quad \dots \quad (5)$$

$$\ddot{r}_t = (\dot{r}_t - \dot{r}_{t-1}) \cdot \Delta t \quad \dots \quad (6)$$

$$\dot{l}_t = (l_t - l_{t-1}) \cdot \Delta t \quad \dots \quad (7)$$

$$l\ddot{\varphi}_{x,t} = \left\{-2\left(\dot{l}\dot{\varphi}_{x,t} - l\dot{\varphi}_t\dot{\varphi}_{y,t}\right) - \left(\frac{k_{D,x}}{m_L}\right)\dot{\varphi}_{x,t}\right\} + \begin{Bmatrix}\left(l\ddot{\varphi}_t\varphi_{y,t}\right) + l\dot{\varphi}_t{}^2\varphi_{x,t} - 2\dot{l}\dot{\varphi}_t\varphi_{y,t} \\ -g\varphi_{x,t} + \left(\frac{\dot{l}_t{}^2}{l_t}\right)\varphi_{x,t}\end{Bmatrix} + \{r_t\dot{\varphi}_t{}^2 - \ddot{r}_t\} \quad \dots \quad (eight)$$

$$\dot{\phi}_{x,t} = \dot{\phi}_{x,t-1} + \ddot{\phi}_{x,t-1} \cdot \Delta t \quad \dots \quad (9)$$

$$\phi_{x,t} = \phi_{x,t-1} + \dot{\phi}_{x,t-1} \cdot \Delta t \quad \dots \quad (10)$$

1. $\varphi_{x,t}$ and $\varphi_{x,t-1}$ are the sway angles along the x direction, respectively, at time t and at the previous time t-1.
2. $\dot{\phi}_{x,t}$ and $\dot{\phi}_{x,t-1}$ are the velocity of the sway angle along the x direction, respectively, at time t and at the previous time t-1.
3. $\ddot{\phi}_{x,t}$ and $\ddot{\phi}_{x,t-1}$ are the accelerations of the sway angle along the x direction, respectively, at time t and at the previous time t-1.
4. $\ddot{r}_t$ is the acceleration of the movement of the trolley relative to the x direction at time t.
5. $\dot{r}_t$ and $\dot{r}_{t-1}$ are the velocity of the movement of the trolley relative to the x direction, respectively, at time t and at the previous time t-1.
6. $\dot{l}_t$ is the velocity of the movement of the hoisting relative to the vertical z direction at time t.
7. l_t and l_{t-1} are the lengths of the cable respectively at time t and at the previous time t-1.
8. Δt is the time difference between the instant t and the instant t-1.

The iterative solution is based on the hypothesis that at the initial instant, the values of the sway angle φ_x, the velocity of the sway angle phi dot sub x, and the acceleration of the

Published By:
Blue Eyes Intelligence Engineering
and Sciences Publication (BEIESP)
© Copyright: All rights reserved.

sway angle $\ddot{\phi}_x$ are equal to zero. That means the pendulum is initially in quiet conditions.
Therefore, for t=0, we have:

$$\phi_{x,0} = \dot{\phi}_{x,0} = \ddot{\phi}_{x,0} = 0 \quad \dots \quad (11)$$

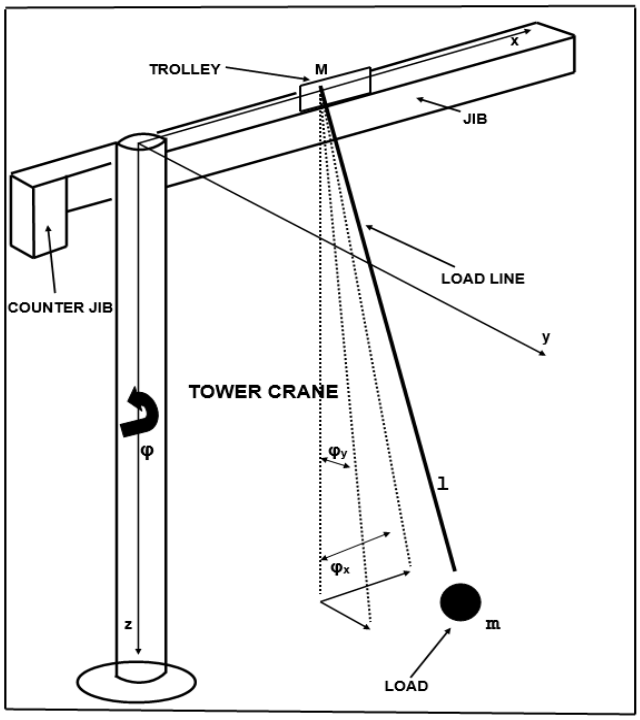

[Fig.2: Geometric Description of the Tower Crane System]

III. KALMAN FILTER

III.1 Notation: We will represent one-dimensional vectors with the "_" symbol underneath, and two-dimensional matrices with the double subscript. The time dependency of the variables is typically not considered for simplicity.

III.2 The Kalman filter tries to estimate, in the presence of disturbances, the internal state $x \in \mathbb{R}^n$, not accessible, of a discrete-time system, whose knowledge of the model is, according to a defined theory, complete. The Kalman filter is the optimal recursive estimator: if the problem noise is Gaussian, the Kalman filter provides a least-squares estimate of the system's internal state. Historically, the Kalman filter is strictly limited to filtering systems where the state transition and observation are linear functions of the current state.

The estimator is simply a tool capable of reconstructing the state of the real system.

In practice, we have two cards to play to reconstruct the state:

1. The mathematical model we have written and whose validity we have demonstrated using model noise.
2. The measurements from the sensors that give us the system's real output (obviously corrupted by noise).

We try to use them consistently to estimate the state.

Following linear systems theory, the dynamics of a continuous-time "linear" system is represented by a differential equation such as:

$$\dot{\underline{x}}(t) = \underline{A}(t)\underline{x}(t) + \underline{B}(t)\underline{u}(t) + \underline{w}(t) \quad \dots (12)$$

state update equation, which is associated with an indirect observation of this state through a linear system:

$$\underline{y}(t) = \underline{H}(t)\underline{x}(t) + \underline{v}(t) \quad \dots \quad (13)$$

where $\underline{y}(t)$ is the vector of observations. The discrete-time Kalman filter comes to the aid of real systems where the system is sampled at discrete intervals, transforming the continuous-time linear system into a linear system of the type:

$$\begin{cases} \underline{x_{k+1}}(t) = \underline{A_k}(t)\underline{x_k}(t) + \underline{B_k}(t)\underline{u_k}(t) + \underline{w_k}(t) \\ \underline{y_k}(t) = \underline{H_k}(t)\underline{x_k}(t) + \underline{v_k}(t) \end{cases} \quad \dots \quad (14)$$

If the system evolves according to this model, it is referred to as a linear-Gaussian state space model or a linear dynamic system. If the matrix values are independent of time, the model is referred to as stationary. The variables $\underline{w_k}(t)$ e $\underline{v_k}(t)$ Represent the process and observation noise, respectively, whose mean value is zero $\underline{\bar{w}_k}(t) \equiv \underline{\bar{v}_k}(t) = 0$ and respective variances $\underline{Q}$ e $\underline{R}$ known (assumed white Gaussian noise). $\underline{A_k}$ is a state transition matrix nxn, $\underline{B_k}$ is a matrix nxl which connects the optional control input $\underline{u_k} \in R^l$ with the state $\underline{x_k}$ and, at the end, $\underline{H_k}$ is a matrix mxn which connects the state with the measure $\underline{y_k}$. All these matrices, representing the system model, must be known with extreme precision; otherwise, systematic errors will be introduced.

The Kalman filter is a recursive estimation filter and requires at each iteration, the knowledge of the state estimated from the previous step $\underline{\hat{x}_{k-1}}$ and the current observation $\underline{y_k}$, i.e., indirect observation of the state of the system.

Let $\underline{\hat{x}_k^-}$ the a priori estimate of the system state, based on the estimate obtained at time $k-1$ and from the dynamics of the problem, and $\underline{\hat{x}_k}$ the estimate of the state of the problem a posteriori of the observation $\underline{y_k}$ and based on it. From these definitions, it is possible to define the a priori and a posteriori estimation error as:

$$\begin{cases} \underline{\hat{e}_k^-} = \underline{x_k} - \underline{\hat{x}_k^-} \\ \underline{\hat{e}_k} = \underline{x_k} - \underline{\hat{x}_k} \end{cases} \quad \dots \quad (15)$$

It is possible to associate the Covariance Matrices, a priori and posterior, respectively, with errors (15):

$$\begin{cases} \underline{\hat{P}_k^-} = \underline{E}[e_k^- e_k^{-T}] \\ \underline{\hat{P}_k} = \underline{E}[e_k e_k^T] \end{cases} \quad \dots \quad (16)$$

The goal of the Kalman filter is to minimise the covariance of the a posteriori error, underbar, denoted as P_k, and provide a method to estimate the state, denoted as x_hat_k, and the observation, denoted as y_k. The Kalman filter provides an a posteriori state estimate through a linear combination of the prior state

© Copyright: All rights reserved.

estimate and the observation error:

$$\underline{\hat{x}_k} = \underline{\hat{x}_k^-} + \underline{K_k}\left(\underline{y_k} - \underline{H_k}\underline{\hat{x}_k^-}\right) \quad \ldots \quad (17)$$

This shifts the problem of estimation to that of deriving the gain factor. $\underline{K_k}$ (Blending factor). The difference $\underline{y_k} - \underline{H_k}\underline{\hat{x}_k^-}$ is called the residual, or innovation, and represents the discrepancy between the predicted observation and the one that actually occurred.

The Kalman filter is typically implemented in two phases: the time update (prediction phase) and the measurement update (observation phase).

In the first phase, the a priori estimate is obtained of both. $\underline{\hat{x}_k}$ and the covariance $\underline{P_k}$. The a priori estimate $\underline{\hat{x}_k^-}$ derives from in-depth knowledge of the system dynamics:

$$\underline{\hat{x}_k^-} = \underline{A_k}\underline{\hat{x}_{k-1}} + \underline{B_k}\underline{u_k} \quad \ldots \quad (18)$$

and the a priori estimate of the error covariance is updated in the same way:

$$\underline{P_k^-} = \underline{A_k}\underline{P_{k-1}}\underline{A_k^T} + \underline{Q_k} \quad \ldots \quad (19)$$

These are the best estimates of the state and covariance of the instant. k obtainable a priori from observing the system.

In the second phase, the gain is calculated, which turns out to be:

$$\underline{K_k} = \underline{P_k^-}\underline{H_k^T}\left(\underline{H_k}\underline{P_k^-}\underline{H_k^T} + \underline{R_k}\right)^{-1} \quad \ldots \quad (20)$$

which minimises the posterior covariance, and with this factor, the posterior state is updated through equation (17). Using this value for the gain $\underline{K_k}$, the a posteriori estimate of the covariance matrix becomes:

$$\underline{P_k} = \left(\underline{I} - \underline{K_k}\underline{H_k}\right)\underline{P_k^-} \quad \ldots \quad (21)$$

To unify the different variants of Kalman filters, we can translate these equations using variance-covariance matrices:

$$\left.\begin{matrix} cov\left(\underline{x_k}, \underline{y_k}\right) = \underline{P_k^-}\underline{H_k^T} \\ cov\left(\underline{y_k}\right) = \underline{H_k}\underline{P_k^-}\underline{H_k^T} \end{matrix}\right\} \quad \ldots \quad (22)$$

so that we can write equation (20) as:

$$\underline{K_k} = cov\left(\underline{x_k}, \underline{y_k}\right)\left(cov\left(\underline{y_k}\right) + \underline{R_k}\right)^{-1} \quad \ldots \quad (23)$$

e l'eq. (21) diventa:

$$\underline{P_k} = \underline{P_k^-} - \underline{K_k}\, cov\left(\underline{x_k}, \underline{y_k}\right)^T \quad \ldots \quad (24)$$

As can be easily seen, the covariance matrix and the Kalman gain do not depend on the state, observations, or residuals, and have an independent history. However, the Kalman filter requires an initial value for the state variable and the covariance matrix. The initial value of the state must be as similar as possible to the actual value, and this similarity must be reflected in the initial covariance matrix.

IV. KALMAN FILTER APPLIED TO THE TOWER CRANE SYSTEM

A. Matrix Equation of the Kalman Filter for the Crane

We can rewrite equations (3) and (4) to obtain matrix equations that will be useful to realize the Kalman filter method. So, from equations. (3) and (4) we get:

$$\ddot{r} - l\varphi_y\ddot{\varphi} + l\ddot{\varphi}_x = (r + l\varphi_x)\dot{\varphi}^2 o - 2\left(\dot{l}\dot{\varphi}_x - l\dot{\varphi}_y\dot{\varphi} - \dot{l}\varphi_y\dot{\varphi}\right) - \left(\frac{k_{D,x}}{m_L}\right)\dot{\varphi}_x - k_{E,x}l\varphi_x + \left\{-g\varphi_x + \left(\frac{l^2}{l}\right)\varphi_x\right\} \quad \ldots \quad (25)$$

$$(r + l\varphi_x)\ddot{\varphi} + l\ddot{\varphi}_y = \left(l\varphi_y\right)\dot{\varphi}^2 o - 2\left(\dot{l}\dot{\varphi}_y + \dot{r}\dot{\varphi} + l\dot{\varphi}_x\dot{\varphi} + \dot{l}\varphi_x\dot{\varphi}\right) - \left(\frac{k_{D,y}}{m_L}\right)\dot{\varphi}_y - k_{E,y}l\varphi_y + \left\{-g\varphi_y + \left(\frac{l^2}{l}\right)\varphi_y\right\} \quad \ldots \quad (26)$$

This allows us to define the matrix equation in Lagrangian coordinates q :

$$\underline{M}\left(\underline{q}\right)\underline{\ddot{q}} + \underline{C}\left(\underline{q}, \underline{\dot{q}}\right)\underline{\dot{q}} + \underline{D}\left(\underline{q}, \underline{\dot{q}}\right)\underline{\dot{q}} + \underline{K}\left(\underline{q}\right) + \underline{G}\left(\underline{q}\right) = \underline{F}\left(\underline{q}, \underline{\dot{q}}\right)\underline{\ddot{q}} \quad \ldots \quad (27)$$

where $\underline{M}$is the mass matrix, $\underline{C}$ the matrix of kinetic forces, $\underline{D}$ the damping matrix due to different factors such as air friction, $\underline{K}$the elastic matrix of the Tower crane structure, $\underline{G}$ the matrix of gravitational terms, $\underline{F}$ the external forces matrix (motors) operating on the Tower crane.

Considering only equations (25) and (26), which relate to the determination of the sway angles as a function of time (where the external forces do not appear), we can obtain the explicit expressions for the terms of equation (27).

$$\underline{M}\left(\underline{q}\right) = \begin{bmatrix} 1 & -l\varphi_y \\ 0 & (r + l\varphi_x) \end{bmatrix}; \begin{bmatrix} l & 0 \\ 0 & l \end{bmatrix} \quad \ldots \quad (28)$$

$$\underline{C}\left(\underline{q}, \underline{\dot{q}}\right)\underline{\dot{q}} = \begin{bmatrix} 0 & -(r + l\varphi_x)\dot{\varphi} \\ 2\dot{\varphi} & -l\varphi_y\dot{\varphi} \end{bmatrix}; \begin{bmatrix} -2\dot{l}\varphi_y & 2\dot{l} \\ 2\dot{l}\varphi_x & 2l\dot{\varphi} \end{bmatrix}; \begin{bmatrix} -2l\dot{\varphi} & 0 \\ 2\dot{l} & 0 \end{bmatrix} \quad \ldots \quad (29)$$

$$\underline{D}\left(\underline{q}, \underline{\dot{q}}\right)\underline{\dot{q}} = \begin{bmatrix} \frac{k_{Dx}}{m_l} \\ \frac{k_{Dy}}{m_l} \end{bmatrix}\begin{bmatrix} \dot{r} & \dot{\varphi} \end{bmatrix} \quad \ldots \quad (30)$$

$$\underline{K}\left(\underline{q}\right) = \begin{bmatrix} k_{Rx}l\varphi_x \\ k_{Ry}l\varphi_y \end{bmatrix} \quad \ldots \quad (31)$$

$$\underline{G}\left(\underline{q}\right) = \begin{bmatrix} g\varphi_x - \frac{\dot{l}^2\varphi_x}{l} \\ g\varphi_y - \frac{\dot{l}^2\varphi_y}{l} \end{bmatrix} \quad \ldots \quad (32)$$

$$\underline{F}\left(\underline{q}, \underline{\dot{q}}\right)\underline{\ddot{q}} = \begin{bmatrix} 0 \\ 0 \end{bmatrix} \quad \ldots \quad (33)$$

B. Kalman Observer for the Tower Crane System

We can turn the matrix equation into the Lagrangian coordinates q, introducing the inverse matrix $\underline{M}^{-1}\left(\underline{q}\right)$, so that we get the following equation, solved as a function of $\underline{\ddot{q}}$:

$$\underline{\ddot{q}} = -\left\{\underline{C}\left(\underline{q}, \underline{\dot{q}}\right)\underline{M}^{-1}\left(\underline{q}\right)\right\}\underline{\dot{q}} + onee\ one - \left\{\underline{D}\left(\underline{q}, \underline{\dot{q}}\right)\underline{M}^{-1}\left(\underline{q}\right)\right\}\underline{\dot{q}} + -\left\{\underline{K}\left(\underline{q}\right) + \underline{G}\left(\underline{q}\right)\right\}\underline{M}^{-1}\left(\underline{q}\right) \quad \ldots \quad (34)$$

Assuming:

Published By:
Blue Eyes Intelligence Engineering
and Sciences Publication (BEIESP)
© Copyright: All rights reserved.

$$\underline{A_0} \triangleq -\left\{\underline{C}\left(\underline{q},\underline{\dot{q}}\right)+\underline{D}\left(\underline{q},\underline{\dot{q}}\right)\right\}\underline{M}^{-1}\left(\underline{q}\right)\underline{\dot{q}} \quad \ldots \quad (35)$$

$$\underline{B_0} \triangleq -\left\{\underline{K}\left(\underline{q}\right)+\underline{G}\left(\underline{q}\right)\right\}\underline{M}^{-1}\left(\underline{q}\right) \quad \ldots \quad (36)$$

$$\underline{x}_m = \underline{\dot{q}} \quad \ldots \quad (37)$$

In this way, we obtain the matrix equation.

$$\underline{\dot{x}}_m = \underline{A_0}\underline{x}_m + \underline{B_0} \quad \ldots \quad (38)$$

Therefore, eq. (38) is the starting equation, which, in our specific case of closed-loop control of the Tower Crane, generates the state update equation (12).

To this, in our case, we add the equation:

$$\underline{y}_m = \underline{H_0}\underline{x}_m + \underline{v} \quad \ldots \quad (39)$$

That is the indirect observation of the state, through the matrix. $\underline{H_0}$, where we consider the cable angles, which are typically estimated through inertial measurements.

Explicitly, we can derive from equations (3) and (4) the explicit matrix equations of the vector $\underline{\dot{x}}_m$, including the state observation equations, through the Kalman filter:

$$\begin{Bmatrix} x_1 = \dot{\varphi}_x \\ x_2 = \dot{\varphi}_y \\ x_3 = \varphi_x \\ x_4 = \varphi_y \end{Bmatrix} \quad \ldots \quad (40)$$

$$l\begin{bmatrix}\dot{x}_1\\ \dot{x}_2\end{bmatrix} = \begin{bmatrix} -2\dot{l} - \left(\frac{k_{D,x}}{m_L}\right) & -2l\dot{\varphi} \\ -2l\dot{\varphi} & -2\dot{l} - \left(\frac{k_{D,y}}{m_L}\right)\end{bmatrix}\begin{bmatrix}x_1\\ x_2\end{bmatrix} +$$

$$+\begin{bmatrix} l\dot{\varphi}^2 - g + \left(\frac{l^2}{l}\right) & l\ddot{\varphi} - 2\dot{l}\dot{\varphi} \\ l\ddot{\varphi} - 2\dot{l}\dot{\varphi} & l\dot{\varphi}^2 - g + \left(\frac{l^2}{l}\right)\end{bmatrix}\begin{bmatrix}x_3\\ x_4\end{bmatrix} + oe +$$

$$\begin{bmatrix} r\dot{\varphi}^2 - \ddot{r} \\ -2\dot{r}\dot{\varphi} - r\ddot{\varphi}\end{bmatrix} \quad \ldots \quad (41)$$

$$\begin{bmatrix}\dot{x}_3\\ \dot{x}_4\end{bmatrix} = \underline{H_0}\begin{bmatrix}x_3\\ x_4\end{bmatrix} \quad \ldots \quad (42)$$

Two IMUs (Inertial Measurement Units), designed for use on the hook system and the tower
tip, should be used in conjunction with the units used for closed-loop velocity control. Both the closed-loop velocity behavior of each drive and the sway angles are controlled..

V. RESULT AND DISCUSSION

At this point, we can define the following iterative procedure for the Kalman-Bucy observer method we applied:

1. We write the model of the real system: eq. (3) and eq. (4).
2. We estimate the model error, i.e., we indicate its variance: eq. (14) and eq. (16).
3. We estimate the measurement error, i.e., we indicate its variance: eq. (14).
4. We calculate the Kalman Gain $\underline{K_k}$ Using an algorithm that takes as input the model matrices and the variances of the model and measurement errors: eq. (19), eq. (20) and eq. (21) using eq. (38) and eq. (39).
5. With this value of $\underline{K_k}$ We minimise the posterior covariance and, with this factor, update the posterior state using equation (17). In our case, the variable estimated through equation (17) is the vector of the Speed references for the Slewing axes and the Trolley.

To test the adopted procedure, we used Codesys V3.5 SP7, written in Structured Language (SL), to simulate the time evolution of the motion equations and define the input casually read by the sensors. An example of the Tower crane parameters used to model the system is described in Table 1.

The Velocity reference is the target speed value, established by the crane operator or the automatic control system at the moment the movement begins. It is defined in Hz, as a consequence of how the electric motors are restricted. In fact, at the speed in Hz on the fast shaft (that is, on the motor), a velocity corresponds on the slow shaft (that is, on the wheels moving on the rails of the trolley or on the shaft controlling the slewing motion of the jib), depending on the reduction gearing from the motor to the wheel.

The Ramp Set represents the time required for the linear motor ramp to reach the speed reference. Based on the speed reference, the system calculates the velocity profile for obtaining the anti-sway effect. Obviously, the speed profile obtained is longer than the linear Ramp Set without the Anti-Sway effect.

Generally, the longer the cable length, the longer the time of the speed profile. In general, it is essential to reduce the time of the velocity profile to provide a fast response to the operator's commands.

Table I: Exemplary Crane Parameters

Symbol	Parameter	Value	Unit
$V_{Ref,\,Sl}$	Slewing Speed reference	30.0	Hz
$V_{Ref,\,Tr}$	Trolley Speed reference	40.0	Hz
$V_{MaxRef,\,Sl}$	Slewing Max Speed reference	50.0	Hz
$V_{MaxRef,\,Tr}$	Trolley Max Speed reference	50.0	Hz
$\dot{\varphi}$	Angular Rotation Velocity	0.1	Rad/s
Acc_{Sl}	Slewing Acc. Ramp Set	5.0	s
Dec_{Sl}	Slewing Dec. Ramp Set	5.0	s
Acc_{Tr}	Trolley Acc. Ramp Set	3.0	s
Dec_{Tr}	Trolley Dec. Ramp Set	3.0	s
l	Cable length	1-50	m
L	Length of the Jib	50	m
l_T	Length of the Tower	50	m
l_{CJ}	Length of the counter-jib	12	m
X_{Tr}	Variable position of the Trolley on the Jib	30	m
m_{CJ}	Counter-Jib mass	$5{\cdot}10^3$	kg
m_L	Load mass	$2{\cdot}10^3$	kg
m_T	Tower mass	$7{\cdot}10^3$	kg
m_{Tr}	Trolley mass	$6{\cdot}10^2$	kg

In the following figures, the values obtained from the simulation in Codesys using the supplied data are represented, yielding the Slewing speed function, which is intended as the Speed

© Copyright: All rights reserved.

Reference for the Slewing axis.

The plots below were obtained by subjecting the considered continuous-time process to two sources of zero-mean Gaussian noise using a random signal generated by a function in the Codesys language.

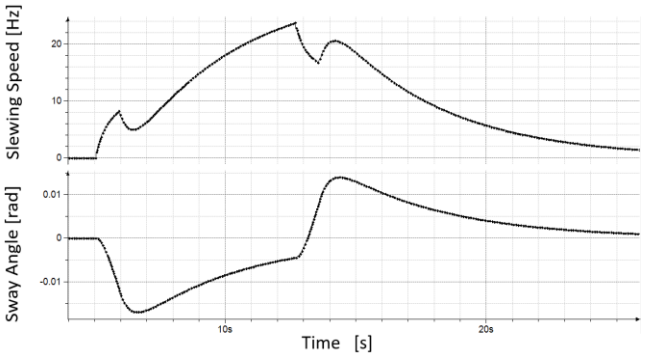

[Fig.3: Profile of the Reference Velocity for the Slewing $\dot{\varphi}$ and the Corresponding Profile for the Perpendicular Sway Angle φ_y Using the Load Anti-Sway Profile. The Initial Slewing Speed Reference = 30 Hz, Ramp Set = 2.5 s, Cable Length = 10.5 m]

In Fig. 3, we represent the profiles of the angular velocity for the slewing movement and the corresponding profile of the tangential sway angle. We can see how the movement ends, the anti-sway effect occurs, and therefore, the swinging of the transported load is also cancelled out.

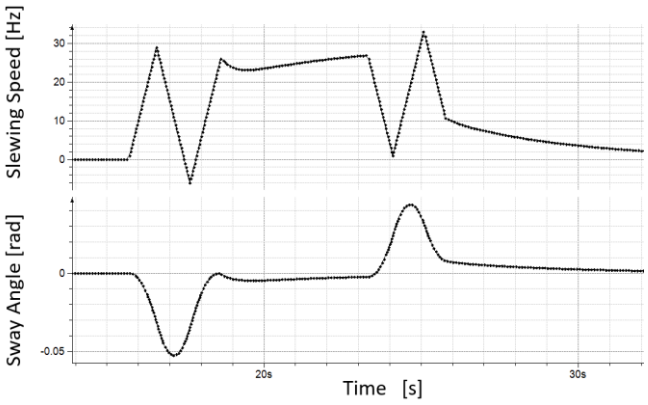

[Fig.4: Profile of the Reference Velocity for the Slewing $\dot{\varphi}$ and the corresponding Profile for the perpendicular sway angle φ_y using the Load Anti-sway profile. The initial Slewing speed reference = 30 Hz, ramp set = 2.5 s, cable length = 10.5 m]

The same profiles are shown in Fig. 4, where, however, the Velocity Reference Profile of the Slewing is calculated using an optimized system to obtain shorter acceleration and deceleration ramps. This way, the system performs better for the operator in terms of response to commands, although it is obviously subject to greater physical stress due to the faster ramps.

In the following figures, we represent the theoretical Velocity reference profile of the Slewing (in black), as shown in Figs. 2 and 3. Along with this profile, two other profiles are represented in the following figures: the profile (in blue) of the Slewing considering the measurement noise (i.e., the measurement errors) and that of the modelling of the phenomenon (i.e., the errors in the modelling of the control of the Slewing crane). Finally, the profile of the Slewing in output is represented (in red), obtained by filtering the signals using the Kalman filter—the vectors. $\underline{w}$and$\underline{v}$, as shown in the equation. (12) and (39), respectively, represent the state variance (Slewing Crane control model) and the output noise variance (input reader noise variance). In this context, the state and output noise are assumed to be zero-mean Gaussian with covariances and respectively.

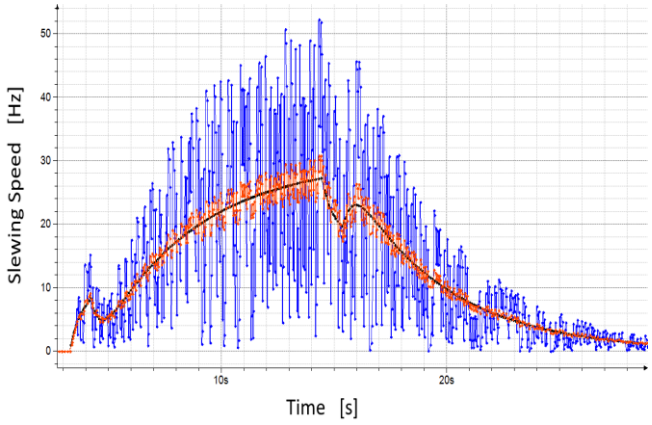

[Fig.5: Profile of the Reference Velocity for the Slewing $\dot{\varphi}$ Using the Input-Shaping Control for the Anti-Vibration System. Theoretical Velocity Reference Profile: Black; State Velocity Reference Profile Considering Model and Output Variances: Blue; Estimated Velocity Reference Profile with Kalman Filter: Red. The Specific Values are: Slewing Speed Reference = 30 Hz, Ramp SET = 2.5 Seconds, Cable Length = 10.5 Meters. Variance of the Output Signal = 0.5; Variance of the Process Equation = 0.5]

In Fig. 5, we can see that, in correspondence with high values of the variances of both the state and the measurement process, a vigorously oscillating profile is obtained on the output (Blue line), which is not very reliable and should be discarded for crane control.

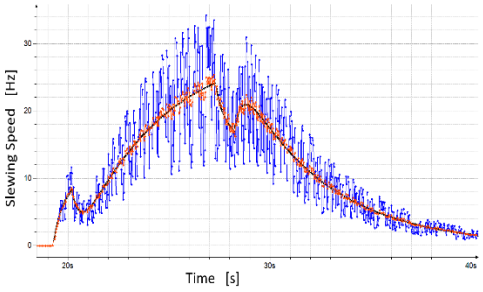

[Fig.6: Profile of the Reference Velocity for the Slewing $\dot{\varphi}$ Using the Input-Shaping Control for the Anti-Vibration System. Theoretical Velocity Reference Profile: Black; State Velocity Reference Profile Considering Model and Output Variances: Blue; Estimated Velocity Reference Profile with Kalman Filter: Red. The Specific Values are: Slewing Speed Reference = 30 Hz, Ramp set = 2.5 Seconds, Cable Length = 10.5 Meters. Variance of the Output Signal = 0.1; Variance of the Process Equation = 0.1]

However, already in Fig.6, we highlight how, in correspondence with improved values of the

Published By:
Blue Eyes Intelligence Engineering
and Sciences Publication (BEIESP)
© Copyright: All rights reserved.

process and output variance, we obtain values on the output (Blue line) with an oscillating profile, but less elevated than in Fig. 5.

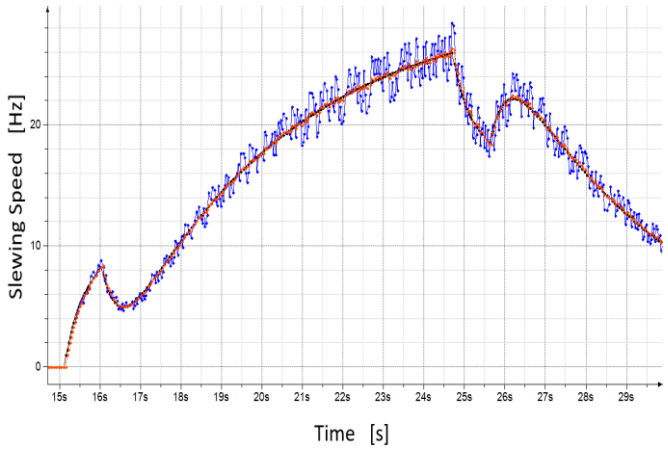

[Fig.7: Profile of the Reference Velocity for the Slewing $\dot{\varphi}$ Using the Input-Shaping Control for the Anti-Vibration System. Theoretical Velocity Reference Profile: Black; State Velocity Reference Profile Considering Model and Output Variances: Blue; Estimated Velocity Reference Profile with Kalman Filter: Red. The Specific Values are: Slewing Speed Reference = 30 Hz, Ramp Set = 2.5 Seconds, Cable Length = 10.5 Meters. Variance of the Output Signal = 0.01; Variance of the Process Equation = 0.1]

In Fig. 7, corresponding to process and output variance values improved by an order of magnitude, significantly less oscillating output profile values (Blue line) are obtained. The profile is thus quite smooth.

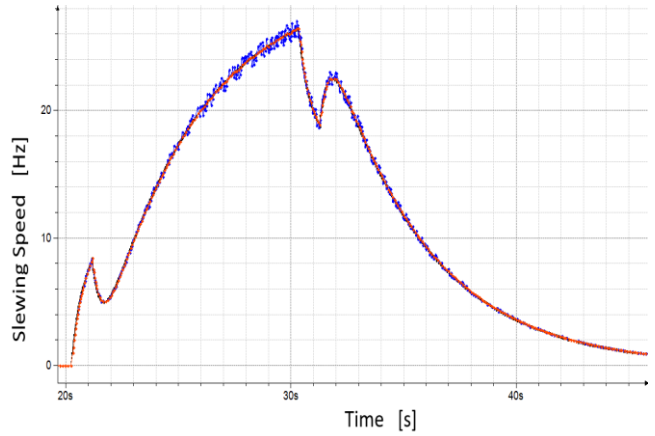

[Fig.8 Profile of the Reference Velocity for the Slewing $\dot{\varphi}$ Using the Input-Shaping Control for the Anti-Vibration System. Slewing Speed Reference = 30 Hz, Ramp set = 2.5 s, Cable Length = 10.5 m. Theoretical Velocity Reference Profile: Black; State Velocity Reference Profile Considering Model and Output Variances: Blue; Estimated Velocity Reference Profile with Kalman Filter: Red. Variance of the Output Signal = 0.01; Variance of the Process Equation = 0.001]

In Fig. 8, corresponding to process variance values further improved by an order of magnitude, even less oscillating output profile values (Blue line) are obtained. The profile is thus already sufficiently smooth.

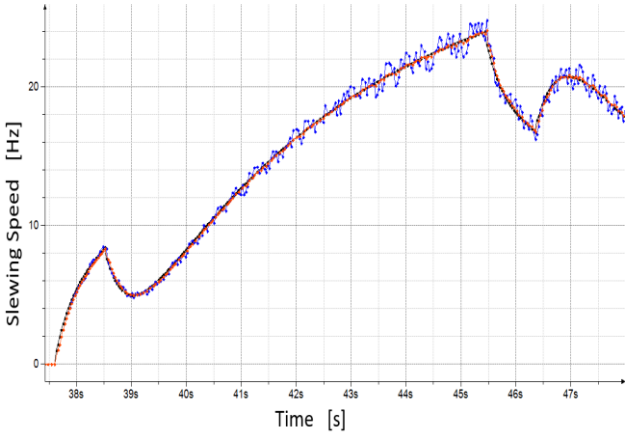

[Fig.9: Profile of the Reference Velocity for the Slewing $\dot{\varphi}$ Using the Input-Shaping Control for the Anti-Vibration System. Slewing Speed Reference = 30 Hz, Ramp Set = 2.5 s, Cable Length = 10.5 m. Theoretical Velocity Reference Profile: Black; State Velocity Reference Profile Considering Model and Output Variances: Blue; Estimated Velocity Reference Profile with Kalman Filter: Red. Variance of the Output Signal = 0.01; Variance of the Process Equation = 0.001]

In Fig. 9, corresponding to process and output variance values that have improved by a further order of magnitude, a really stable output profile is obtained (Blue line). The profile is thus extremely smooth.

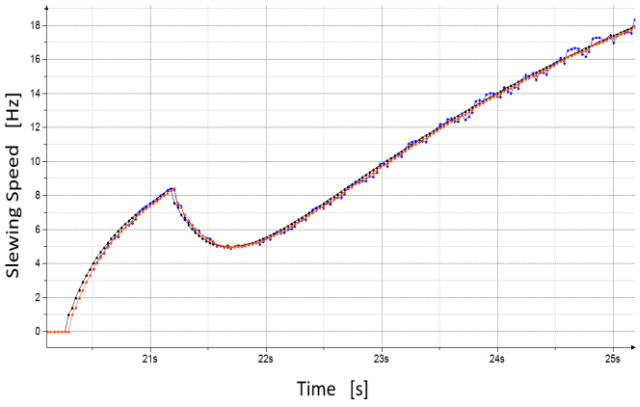

[Fig.10 An Initial Part of the Velocity Reference Profile of the Slewing $\dot{\varphi}$ Using the Input-Shaping Control for the Anti-Vibration System. Theoretical Velocity Reference Profile: Black; State Velocity Reference Profile Considering Model and Output Variances: Blue; Estimated Velocity Reference Profile with Kalman Filter: Red. The Specific Values are: Slewing Speed reference = 30 Hz, Ramp Set = 2.5 Seconds, Cable Length = 10.5 Meters. Variance of the Output Signal = 0.001; Variance of the Process Equation = 0.001]

The fact that the profile is exceptionally smooth, with very low variance values (0.001), is evident in Fig. 10, where a portion of the curve is

© Copyright: All rights reserved.

represented to precisely highlight the regularity of the output profile (Blue line).

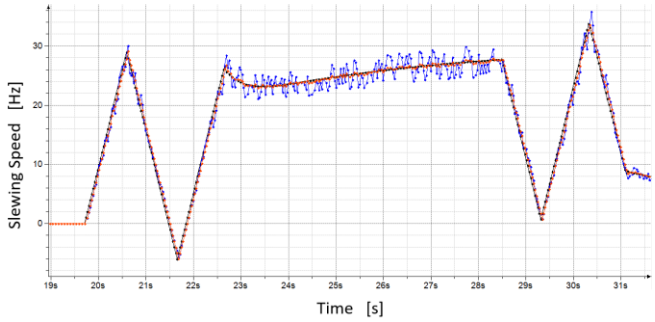

[Fig.11 Profile of the Reference Velocity for the Slewing $\dot{\varphi}$ Using the Input-Shaping Control for the Anti-Vibration System with Optimized Profile. Theoretical Velocity Reference Profile: Black; State Velocity Reference Profile Considering Model and Output Variances: Red; Estimated Velocity Reference Profile with Kalman Filter: Blue. Slewing Speed Reference = 30 Hz, Ramp Set = 2.5 s, Cable Length = 10.5 m. Variance of the Output Signal = 0.01; Variance of the Process Equation = 0.001]

Finally, Fig. 11 illustrates an example of an optimised profile representation of the Velocity Reference, achieved by increasing the ramp speed to optimise the response times of the anti-sway system. We can also see, in this case, how, in correspondence with extremely low process and output variance values, very stable output profile values (Blue line) are obtained. The profile is thus extremely smooth and therefore correct.

VI. CONCLUSION

In this paper, we developed a method for creating a Velocity profile for an Industrial Tower Crane, controlled in closed-loop with Anti-Sway, using a Kalman Filter. This is to reduce the errors introduced by the developed method.

The natural development of the method described in this work is achieved by introducing, in the Lagrange equations that describe the movement of the jib crane, the variation due to the vibrations generated by the elastic and non-rigid structure of the tower jib crane.

DECLARATION STATEMENT

I must verify the accuracy of the following information as the article's author.

- **Conflicts of Interest/ Competing Interests:** Based on my understanding, this article has no conflicts of interest.
- **Funding Support:** This article has not been funded by any organisations or agencies. This independence ensures that the research is conducted with objectivity and without any external influence.
- **Ethical Approval and Consent to Participate:** The content of this article does not necessitate ethical approval or consent to participate with supporting documentation.
- **Data Access Statement and Material Availability:** The adequate resources of this article are publicly accessible.
- **Author's Contributions:** The authorship of this article is contributed solely by the author.

REFERENCES

1. Ramli L., Mohamed Z., Abdullahi A.M., Jaafar H.I., and Lazim, I.M. (2017). Control strategies for crane systems: A comprehensive review. *Mech.Syst. Signal Pr.*, 95, 1–23. DOI: http://dx.doi.org/10.1016/j.ymssp.2017.03.015
2. A. Alfadhli and E. Khorshid, "Payload Oscillation Control of Tower Crane Using Smooth Command Input", *Journal of Vibration and Control*, 2021. DOI: http://doi.org/10.1177/10775463211054640
3. J.H. Montonen, N. Nevaranta, M. Niemelä and T. Lindh." Comparison of Extrainsensitive Input Shaping and Swing-Angle-Estimation-Based Slew Control Approaches for a Tower Crane", *Applied Sciences*. 2022, Vol . 12. pp. 5945. DOI: http://doi.org/10.3390/app12125945
4. M. Zhang, Y.F. Zhang, H. Ouyang, C. Ma and X. Cheng, "Adaptive integral sliding mode control with payload sway reduction for 4-DOF tower crane systems", *Nonlinear Dynamics*, 2020, Vol. 99. DOI: http://doi.org/10.1007/s11071-020-05471-3
5. S. Dutta, Y. Cai, and J. Zheng. "Multi-objective Anti-swing Trajectory Planning of Double-pendulum Tower Crane Operations using Opposition-based Evolutionary Algorithm". *ArXiv,* 2023. DOI: http://doi.org/10.48550/arXiv.2305.18745
6. Roberto P. L. Caporali, "Iterative Method for controlling the sway of a payload on tower (slewing) cranes using a command profile approach", *International Journal of Innovative Computing, Information and Control*, 2018, Vol. 14, 4, 1169-1187. DOI: http://doi.org/10.24507/ijicic.%2014.04.1169
7. Roberto P. L. Caporali, "Anti-Sway control on a Harbour Crane system using a Command Smoothing iterative method", *International Journal of Innovative Research & Development*, 2022, Vol. 11, 7, 21-31. DOI: http://doi.org/10.24940/ijird/2022/v11/i7/JUL22007
8. F. Liu, J. Yang, J. Wang and C. Liu, "Swing Characteristics and Vibration Feature of Tower Cranes under Compound Working Condition", *Hindawi Shock and Vibration*, 2021. DOI: http://doi.org/10.1155/2021/8997396
9. M.H. Ghawzani, A.H. Alnujaie, M.L. Chandravanshi, D. Deepak, C. Singh, M. Kumar, Y.S. Choo and F.S. Cui, "Failure Analyses of Tower Crane using FEM and theoretical studies", *Journal of Mechanical Design and Vibration*, 2019, Vol. 7, No. 1, 33-DOI: https://doi.org/10.53370/001c.36800
10. F. Rauscher and O. Sawodny, "An Elastic Jib Model for the Slewing Control of Tower Cranes", *Science Direct IFAC PapersOnline*, 2017, Vol. 50-1, pp.9796-9801. DOI: https://doi.org/10.1016/j.ifacol.2017.08.886
11. Roberto P. L. Caporali, "Anti-sway method for reducing vibrations on a tower crane structure", *International Journal of Nonlinear Sciences and Numerical Simulation*, 2021, DOI: https://doi.org/10.1515/ijnsns-2021-0046
12. Roberto P. L. Caporali, "Vibration Normal Modes of a Jib Crane Modelled as an Euler–Bernoulli boom using FEM", *International Journal of Basic Sciences and Applied Computing,* 2023, DOI: https://doi.org/10.35940/ijbsac.D0509.1210423
13. Roberto P. L. Caporali, "Vibration Analysis and Motion Control Method for an Under-Actuated Tower Crane", *International Journal of Inventive Engineering and Sciences,* 2024, DOI: http://doi.org/10.35940/ijies.A1088.11010124
14. A. Pezhman, M. Masoumnezhad, and V. Nouraifar, "Optimise the motion model of overhead crane with an accurate estimate of the equation of state variables by using Unscented Kalman Filter", *3rd International Conference on Research in Science and Technology*, 2016, Berlin. https://scholar.google.com/citations?view_op=view_citation&hl=en&user=ySJsC7MAAAAJ&citation_for_view=ySJsC7MAAAAJ:u-x6o8ySG0sC.
15. K. Jaehoon, K. Balint, K. Donggil and L. Dongik, "Tracking Control of Overhead Crane Using Output Feedback with Adaptive Unscented Kalman Filter and Condition-Based Selective Scaling", *IEEE Access 9:108628-108639*, Vol . 12, pp. 5945, 2021. DOI: http://doi.org/10.1299/mey.22-00231
16. C. Zhimei, W. Jiakai, S. Xuejuan, W. Zhenyan and Z. Yinggang, "Positioning of Tower Crane Trolley Based on D-S Evidence

© Copyright: All rights reserved.

Theory and Kalman Filter", *Mathematical Problems in Engineering*, 2022. DOI: http://doi.org/10.1155/2022/4208045
17. M. Thomas, T. Englert and O. Sawodny, "Model-based velocity-tracking-control of self-erecting industrial tower cranes", *Control Engineering Practice*, 2024, DOI: http://doi.org/10.1016/j.conengprac.2024.105928
18. Roberto P. L. Caporali, "Classical and Quantum Kalman Filter: an application to an Under-actuated Nonlinear System as a Gantry crane", *International Journal of Recent Engineering Research and Development,* 2022, http://ijrerd.com/volume7-issue4.htm

AUTHOR'S PROFILE



Roberto P. L. Caporali was born in Milano in 1963. He received the M.S. degree in Nuclear Engineering from Politecnico di Milano. Between 1996 and 2015, he worked in companies involved in mechatronics applications. In 2015, he founded his company to develop Patents and Mathematics Applications for Engineering. He created works in various fields, including Automatic Control, Advanced Control Theory, Quantum Statistical Mechanics, Quantum Computing, and Condensed Matter. An exhaustive list of the author's published papers appears on ResearchGate. Reviewer in Scopus-indexed publications: Mechanical & Materials Engineering, SN Computer Science.

Disclaimer/Publisher's Note: The statements, opinions and data contained in all publications are solely those of the individual author(s) and contributor(s) and not of the Blue Eyes Intelligence Engineering and Sciences Publication (BEIESP)/ journal and/or the editor(s). The Blue Eyes Intelligence Engineering and Sciences Publication (BEIESP) and/or the editor(s) disclaim responsibility for any injury to people or property resulting from any ideas, methods, instructions, or products referred to in the content.

© Copyright: All rights reserved.